ELSEVIER

Powder Technology 99 (1998) 132–139

POWDER TECHNOLOGY

Dynamics of collapsing fluidized beds and its application in the simulation of pulsed fluidized beds

Yongsheng Nie *, Dayou Liu

Institute of Mechanics, Chinese Academy of Sciences, Beijing, China

Received 20 March 1998; received in revised form 4 June 1998

Abstract

A new method to study collapsing process of fluidized bed was proposed. The method is based on the analysis of the pressure variation during collapse. A model is proposed to describe the pressure variation on any location of the bed during collapse. Three kind of particles were fluidized by air and the pressure variation after shutting down the gas supply was measured by pressure transducers and simulated by the proposed model. The simulated results were in good agreement with the experimental data. The parameters of the fluidized bed, such as bubble fraction α_b, particle fraction in dense phase α_p, bubble velocity u_b and slip velocity of particle u_t, can be estimated from the measured pressure data by using the proposed model. The model was also used to calculate the pressure variation in pulsed fluidized beds with low frequency. © 1998 Elsevier Science S.A. All rights reserved.

Keywords: Bed collapse; Pressure; Model; Pulsed fluidized beds

1. Introduction

Bed collapsing technique has been widely used to study the behavior of a fluidized bed. It is attractive because of its simplicity and its potential for rapid determination. A number of workers have applied it for the measurement of the properties of dense phase and bubbles in bubbling fluidized beds, such as dense phase voidage [1–3]; sedimentation velocity and expansion ratio of the dense phase [4]; and fraction and rising velocity of bubbles [5]. It has also been used in powder classification and evaluation of the quality of fluidization [6].

At present, the primary method to study collapsing process is by following the movement of the bed surface by photographic techniques after a sudden termination of the gas supply and the pictures need to be analyzed one by one, then the variation of the bed surface location can be plotted [1–4]. This is a time consuming procedure. An optical-fibre tracking set was developed by the Institute of Chemical Metallurgy, Academia Sinica which made the measurement more convenient and precise, but the device is complex and expensive [7].

In our work, pressure transducers were used to record the pressure variation during the collapsing process. Measuring the pressure variation is a better way to study collapse because it is simpler and faster than other methods. In this paper, we will analyze the collapsing process and propose a model to describe the pressure variation during the collapsing process, then use the model to estimate the parameters of fluidized bed and simulate the collapsing process.

The gas–solid contact efficiency can be much improved in pulsed fluidized beds [8,9], however little work has been done on the dynamics of pulsed fluidized beds. We carried out a study of pulsed fluidized beds recently and will use the proposed model to simulate the pressure variation in pulsed fluidized beds with low frequency.

2. Mathematical model

When the gas supply of the fluidized bed is shut off abruptly at $t=0$, the bed height will vary with time as shown in Fig. 1. At first, bubbles ascend through the bed, leading to

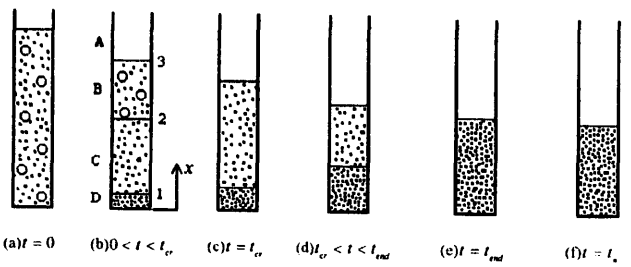

Fig. 1. The collapsing process of bubbling fluidized bed.

* Corresponding author

0032-5910/98/$ - see front matter © 1998 Elsevier Science S.A. All rights reserved.
PII S0032-5910(98)00096-5

rapid collapse of the bed, this stage is called bubble escape stage ($0<t<t_{cr}$). During this stage the upper section of the bed consists of bubbles, below it is a bubble-free dense phase and at the bottom of the bed is the accumulated layer built by the settled particles. At $t=t_{cr}$, bubbles disappear completely, thereafter the bed surface continues to descend while the accumulated layer at the bottom ascends ($t_{cr}<t<t_{end}$). At $t=t_{end}$, all the gas in the dense phase has been expelled and the collapse process is complete. (Strictly, the bed height should descend even more owing to the consolidation of the particles, until at $t=t_\infty$ the ultimate height is reached).

We can divide the fluidized bed during the collapsing process into four regions as shown in Fig. 1(b):

Region A: the region above the bed surface;

Region B: the upper section consisting of bubbles, emulsion phase (or called dense phase) and wake;

Region C: bubble-free dense phase;

Region D: accumulated layer built by the settled particles.

The interfaces of the neighboring two regions are called surface 1, surface 2 and surface 3 and their location are x_{s1}, x_{s2} and x_{s3} respectively.

Our model is based on the following assumption:

(i) the fluidized bed is made up of a bubble phase devoid of particles, emulsion phase and wake;

(ii) all the particles have a uniform dimension;

(iii) bubbles are distributed uniformly in the whole bed with the same rising velocity u_b;

(iv) at any time, the bubble fraction in region B is α_b, the wake fraction is α_w, the particle fraction in the wake phase and the dense phase in region B and C is α_p, the velocity of particles in the wake is the same as the rising velocity of bubble;

(v) the consolidation of the settled particles is neglected and the fraction of particle in accumulated layer is α_∞;

(vi) the density of gas is constant.

2.1. Location variation of the interfaces

Firstly, the location variation of the three interfaces will be derived.

In region B, if the velocity of dense phase is u_e, then

$$\alpha_b u_b+\alpha_w u_b+(1-\alpha_b-\alpha_w)u_e=u_f \tag{1}$$

The derivation of Eq. (1) is shown in Appendix A. u_f is the releasing rate of the gas in the plenum chamber and can be calculated by Eq. (2) [5].

$$u_f=\left(\frac{W}{A}+\Delta P_d\right)\frac{V_0}{AP_a t_{end}} \tag{2}$$

In the dense phase of region B, if $u_{g,B}$ is the gas velocity and $u_{p,B}$ is the average velocity of particles, then

$$(1-\alpha_p)u_{g,B}+\alpha_p u_{p,B}=u_e \tag{3}$$

Additionally, the relationship between the velocities of particle and gas is:

$$u_{g,B}-u_{p,B}=u_t \tag{4}$$

Where, $u_t=u_t(\alpha_p)$, is the slip velocity of particle, Eqs. (1), (3) and (4) give:

$$u_{p,B}=-\frac{(\alpha_b+\alpha_w)u_b-u_f}{1-\alpha_b-\alpha_w}-(1-\alpha_p)\mu_t \tag{5}$$

In region C:

$$(1-\alpha_p)u_{g,C}+\alpha_p u_{p,C}=u_f \tag{6}$$

$$u_{g,C}-u_{p,C}=u_t \tag{7}$$

So,

$$u_{p,C}=u_f-(1-\alpha_p)u_t \tag{8}$$

2.1.1. $0\le t\le t_{cr}$

When $t<t_{cr}$, the mass balance relations of solid phase at the three interfaces are:

$$\text{Surface 1: } \left(u_{p,C}-\frac{dx_{s1}}{dt}\right)\alpha_p=\left(u_{p,D}-\frac{dx_{s1}}{dt}\right)\alpha_\infty \tag{9}$$

$$\text{Surface 2: } \left(u_{p,w}-\frac{dx_{s2}}{dt}\right)\alpha_w\alpha_p+\left(u_{p,B}-\frac{dx_{s2}}{dt}\right)\times(1-\alpha_b-\alpha_w)\alpha_p=\left(u_{p,C}-\frac{dx_{s2}}{dt}\right)\alpha_p \tag{10}$$

$$\text{Surface 3: } \left(u_{p,A}-\frac{dx_{s3}}{dt}\right)\times 0=\left(u_{p,w}-\frac{dx_{s3}}{dt}\right)\alpha_w\alpha_p+\left(u_{p,B}-\frac{dx_{s3}}{dt}\right)(1-\alpha_b-\alpha_w)\alpha_p \tag{11}$$

Where $u_{p,w}$ is the velocity of the particles in wake, $u_{p,w}=u_b$; $u_{p,A}$, $u_{p,D}$ are the average velocity of particles in Region A and Region D respectively, $u_{p,D}=0$.

Replacing $u_{p,B}$ and $u_{p,C}$ in Eqs. (9)–(11) with Eqs. (5) and (8) and integrating Eqs. (9)–(11) under the following initial conditions: $x_{s1}(0)=0, x_{s2}(0)=0, x_{s3}(0)=H_0$, we get:

$$x_{s1}=\frac{[(1-\alpha_p)u_t-u_f]\alpha_p t}{\alpha_\infty-\alpha_p} \tag{12}$$

$$x_{s2}=u_b t-(1-\alpha_p)\left(1+\frac{\alpha_w}{\alpha_b}\right)u_t t \tag{13}$$

$$x_{s3}=H_0-\frac{[\alpha_b u_b-u_f+(1-\alpha_b-\alpha_w)(1-\alpha_p)u_t]t}{1-\alpha_b} \tag{14}$$

When $t=t_{cr}$, surface 3 is at the same location with surface 2, that is $x_{s3}=x_{s2}$, so:

$$t_{cr}=\frac{H_0\alpha_b(1-\alpha_b)}{u_b\alpha_b-\alpha_w(1-\alpha_p)u_t-u_f\alpha_b} \tag{15}$$

$$x_{s3}|_{t=t_{cr}}=x_{s2}|_{t=t_{cr}} \tag{16}$$
$$=\frac{H_0(1-\alpha_b)\alpha_b u_b-(1-\alpha_p)(\alpha_b+\alpha_w)u_t}{(u_b-u_t)\alpha_b-\alpha_w(1-\alpha_p)u_t}$$

2.1.2. $t>t_{cr}$

When $t>t_{cr}$, the mass balance on surface 2 becomes:

$$\left(u_{p,A}-\frac{dx_{s2}}{dt}\right)\times 0=\left(u_{p,C}-\frac{dx_{s2}}{dt}\right)\alpha_p \tag{17}$$

Taking Eq. (16) as the initial condition, Eq. (17) can be integrated:

$$x_{s2}=H_0(1-\alpha_b)-(1-\alpha_p)u_t t+u_t t \tag{18}$$

On surface 1, the mass balance relation is still expressed by Eq. (9) and its location variation can still be expressed by Eq. (12).

When $t=t_{end}$, $x_{s1}=x_{s2}$, so:

$$t_{end}=\frac{H_0(1-\alpha_b)(\alpha_z-\alpha_p)}{\alpha_z(1-\alpha_p)u_t-u_t\alpha_z} \tag{19}$$

$$x_{s1}|_{t=t_{end}}=x_{s2}|_{t=t_{end}}=\frac{H_0\alpha_p(1-\alpha_b)}{\alpha_z}=H_s \tag{20}$$

Fig. 2 is the typical plot of the location variation of the three interfaces with time. In the figure, line mpqs, opqs, and oqs correspond to surface 3, surface 2 and surface 1 respectively.

2.2. Pressure variation

Now we will derive the pressure variation with time at a horizontal which is at a distance x from the distributor. The momentum equations of the gas phase and the solid phase give the following (see Appendix B).

For region B and C:

$$\frac{dp}{dx}=-(1-\varepsilon)\rho_p g. \tag{21}$$

For region D:

$$\frac{dp}{dx}=-Ku_t, \tag{22}$$

where,

$$K=\frac{180\mu_g\alpha_z^2}{d_p^2(1-\alpha_z)^3} \tag{23}$$

Integrating Eqs. (21) and (22) from x to the bed surface gives the pressure distribution $p(t,x)$ (in this article, it is the relative pressure).

When $t<t_{cr}$,

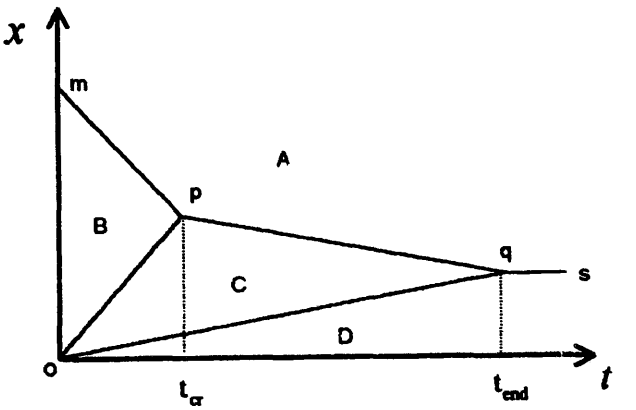

Fig. 2. Typical plot of the location variation of the three interfaces with time.

$$\frac{p(t,x)}{\alpha_p\rho_p g}=$$

$$\begin{cases}0 & (x>x_{s3})\\ (H_0-x)(1-\alpha_b)+(u_t-\alpha_b u_b)t-(1-\alpha_b-\alpha_w)(1-\alpha_p)u_t t & (x_{s2}<x\le x_{s3})\\ H_0(1-\alpha_b)-(1-\alpha_p)u_t t+u_t t-x & (x_{s1}<x\le x_{s2})\\ H_0(1-\alpha_b)-\dfrac{[(1-\alpha_p)u_t-u_t](\alpha_z\rho_p g-Ku_t)\alpha_p t+Ku_t x(\alpha_z-\alpha_p)}{(\alpha_z-\alpha_p)\alpha_p\rho_p g} & (0\le x\le x_{s1})\end{cases} \tag{24}$$

When $t\ge t_{cr}$

$$\frac{p(t,x)}{\alpha_p\rho_p g}=$$

$$\begin{cases}0 & (x>x_{s2})\\ H_0(1-\alpha_b)-(1-\alpha_p)u_t t+u_t t-x & (x_{s1}<x\le x_{s2})\\ H_0(1-\alpha_b)-\dfrac{[(1-\alpha_p)u_t-u_t](\alpha_z\rho_p g-Ku_t)\alpha_p t+Ku_t x(\alpha_z-\alpha_p)}{(\alpha_z-\alpha_p)\alpha_p\rho_p g} & (0\le x\le x_{s1})\end{cases} \tag{25}$$

Our experiments and calculation showed that, in most case, especially when the volume of the plenum was small, u_t was very small and had little influence on the pressure calculation, so it can be neglected and Eqs. (24) and (25) are simplified as follows:

When $t<t_{cr}$,

$$\frac{p(t,x)}{\alpha_p\rho_p g}=$$

$$\begin{cases}0 & (x>x_{s3})\\ (H_0-x)(1-\alpha_b)-\alpha_b u_b t-(1-\alpha_b-\alpha_w)(1-\alpha_p)u_t t & (x_{s2}<x\le x_{s3})\\ H_0(1-\alpha_b)-(1-\alpha_p)u_t t-x & (x_{s1}<x\le x_{s2})\\ H_0(1-\alpha_b)-\dfrac{(1-\alpha_p)\alpha_z u_t t}{\alpha_z-\alpha_p} & (0\le x\le x_{s1})\end{cases} \tag{26}$$

When $t\ge t_{cr}$,

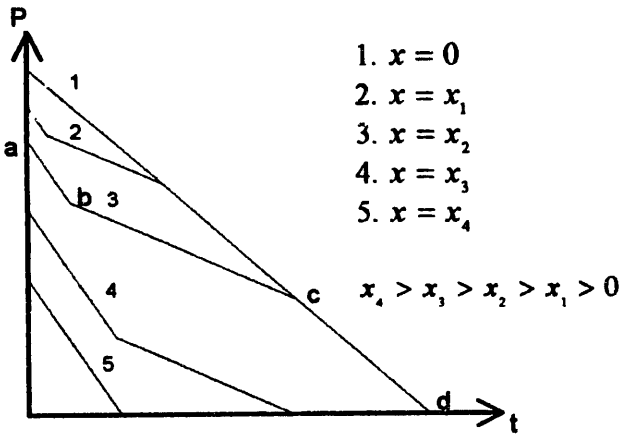

Fig. 3. Plot of $p(t)$ at different location of the bed during collapse.

$$\frac{p(t,x)}{\alpha_p\rho_p g}=\begin{cases}0 & (x>x_{s2})\\ H_0(1-\alpha_b)-(1-\alpha_p)u_t t-x & (x_{s1}<x\le x_{s2})\\ H_0(1-\alpha_b)-\dfrac{(1-\alpha_p)\alpha_z u_t t}{\alpha_z-\alpha_p} & (0\le x\le x_{s1})\end{cases} \tag{27}$$

α_z in the model can be obtained by measuring the static bed height H_s and weighing the particles in the column, H_0 can be measured before collapsing. Thus there are five parameters to be determined in the model α_b, α_w, u_b, α_p and u_t, and among them there are only four independent ones, because

$$H_0(1-\alpha_b)\alpha_p=H_s\alpha_z \tag{28}$$

The pressure distribution $p(t, x)$ can be calculated by Eqs. (24) and (25) or Eqs. (26) and (27) provided that the parameters are known.

Fig. 3 is the pressure variation with time at different location of the bed during collapse according Eqs. (24) and (25). We can see that three kinds of straight lines with different slope appear on the curves. Taking the curve at $x=x_2$ as an example, line *ab* corresponds to the pressure before surface 2 reaches this location and its slope can be calculated from Eq. (24):

$$k_1=\left.\frac{dp}{dt}\right|_{ab}=-[(1-\alpha_b-\alpha_w)(1-\alpha_p)u_t+\alpha_b u_b-u_f]\alpha_p\rho_p g \tag{29}$$

Line *bc* corresponds to the pressure after surface 2 reaches this location and before surface 1 reaches this location, its slope is given by Eq. (24) or Eq. (25):

$$k_2=\left.\frac{dp}{dt}\right|_{bc}=-[(1-\alpha_p)u_t-u_f]\alpha_p\rho_p g \approx-(1-\alpha_p)u_t\alpha_p\rho_p g \tag{30}$$

Line *cd* corresponds to the pressure after surface 1 reaches this location and its slope is given by Eq. (24) or Eq. (25):

$$k_3=\left.\frac{dp}{dt}\right|_{cd}=-\frac{[u_t(1-\alpha_p)-u_f](\alpha_z\rho_p g-Ku_t)\alpha_p}{\alpha_z-\alpha_p} \approx-\frac{\alpha_z(1-\alpha_p)u_t\alpha_p\rho_p g}{\alpha_z-\alpha_p} \tag{31}$$

On the pressure curves of different location, the lines with slope k_1 are parallel and so are the lines with slope k_2, the lines with slope k_3 almost overlap on the same line.

Eqs. (30) and (31) give $(|k_3|)/(|k_2|)=(\alpha_z)/(\alpha_z-\alpha_p)>1$, that is, $|k_3|>|k_2|$. During the period after surface 2 reaches the location and before surface 1 reaches the location, what leads to the pressure variation is the descent of surface 2; After surface 1 reaches the location, both the descent of surface 2 and the ascent of surface 1 affects the pressure variation. So pressure descends faster after surface 1 reaches the location than before surface 1 reaches the location, namely, $|k_3|>|k_2|$.

It has been reported that the voidage of dense phase and the interstitial gas velocity can be obtained by following the variation of the bed height during collapse [1,2]. Similarly, the parameters of a fluidized bed can also be obtained by measuring the pressure variation during collapse.

The particle fraction in dense phase α_p and the slip velocity of particle u_t can be calculated by using Eqs. (30) and (31) after we know slope k_2 and k_3 from the pressure variation curves obtained experimentally, the bubble fraction α_b can then be calculated by using Eq. (28).

In order to calculate u_b, taking $\alpha_b=3\alpha_w$ [10], then u_b can be obtained by using Eq. (29) after we know k_1 from the experimental curves.

3. Experimental

Fig. 4 is the schematic diagram of the experimental apparatus. The experiments were carried out under ambient conditions in a 70 mm ID and 870 mm height perspex column fitted with a porous plate distributor. The pressures in the plenum chamber and on different location of the bed were measured simultaneously by five pressure transducers and the signal was collected and treated by a computer after mag-

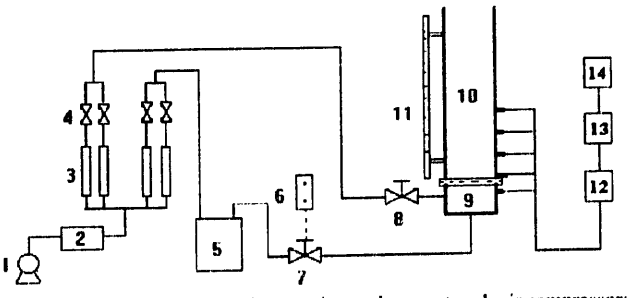

Fig. 4. Schematic diagram of the experimental apparatus: 1, air compressor; 2, dryer; 3, rotameter; 4, needle valve; 5, surge tank; 6, time-lag relay; 7 and 8, solenoid valve; 9, plenum chamber; 10, fluidized bed; 11, ruler; 12, pressure transducer; 13, A/D converter; 14, Computer.

Table 1
Physical properties of the solid used

Particle	d_p (μm)	ρ_p (kg/m^3)	u_{mf} (m/s)
FCC-I	70	1598	0.007
FCC-II	50	1020	0.001
Sand	210	2600	0.030

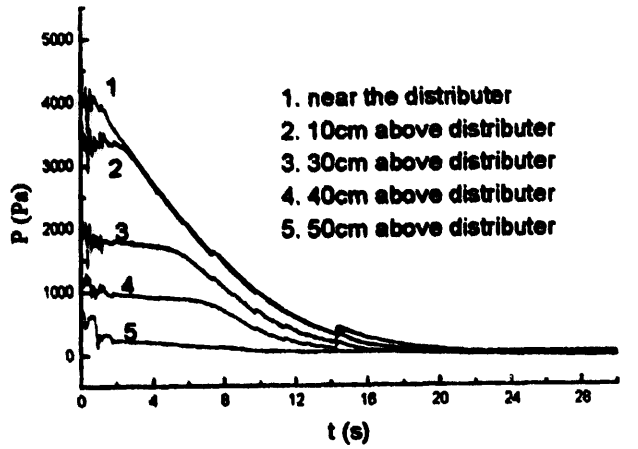

Fig. 5. Measured pressure variation during collapse: (1800 g FCC-I, $u_g = 4u_{mf}$).

nification and A/D conversion. The gas used was air. The solids used and their properties are shown in Table 1.

3.1. Bed collapse

Particles were fluidized at a certain gas velocity and the initial bed height H_0 was measured, then the gas supply was terminated by turning off the solenoid valve and the pressure was recorded. The static bed height H_s was measured after collapsing completed. The sampling frequency is 100 Hz. One of the measured pressure curves is shown in Fig. 5.

3.2. Pulsed fluidization

Particles were fluidized by pulsed gas. The average gas velocity was controlled by the rotameter, the pulse frequency and the duration ratio were controlled by the graded time-lag relay. The pressure variations at different bed location were recorded by pressure transducers and the sampling frequency was 100 Hz.

4. Results and discussion

4.1. Parameters estimation from the pressure curves

Comparing Figs. 3 and 5, we can see that the measured pressure variation curves are very similar to the curves calculated by using the model. α_b, α_p, u_b and u_t can be estimated after the slopes of the lines on the curves are measured.

Table 2
Results of the estimation of fluidization parameters

Particle	u_g (m/s)	α_b	u_b (m/s)	α_p	u_t (m/s)
FCC-I	0.014	0.01	?	0.53	0.008
	0.028	0.09	0.29	0.53	0.008
	0.070	0.11	0.40	0.53	0.008
FCC-II	0.007	0.06	?	0.48	0.005
Sand	0.10	0.16	?	0.52	0.18

On the measured curves, the segment, which should be a line with slope k_1, is not a straight line due to the fierce pressure fluctuation during the bubble escape stage. k_1 can be obtained by line-fitting of the experimental data and the experiments should be repeated for several times under the same conditions in order to improve the precision.

The estimated results of a fluidized bed with different particles and different gas velocity are shown in Table 2. In some tests, u_b is not obtained because of the difficulty of calculating k_1.

4.2. Simulation of collapsing process

The collapsing process can be simulated by using the proposed model if α_b, α_w, u_b, α_p and u_t are given (only four parameters are independent).

Fig. 6 is the comparison between the simulated and measured pressure variation on different locations of the bed. We can see that the simulated results are in good agreement with the measured results except for the period near the completion of collapse.

4.3. Simulation of pulsed fluidized bed

If the pulse frequency is low, during the on-period of the pulsed fluidization, the bed is in a state of fluidization. During the off-period, it is a bed-collapsing process. Therefore the pressure variation during the off-period can be calculated by Eqs. (24) and (25). During the on-period, a certain time is needed to establish the steady state of fluidization and the bed height varies considerably. Meanwhile, the pressure fluctuates greatly due to the existence of bubbles. If the pulse frequency is low, the time for the establishment of the steady fluidization is relatively short. For simplicity, we neglect the period for establishing steady fluidization and assume that the bed height and the pressure are steady, so the pressure at a distance x from the distributor during on-period can be calculate by the following equation:

$$p(x)=(H_0-x)(1-\alpha_b)\alpha_p\rho_p g \tag{32}$$

Then the pressure variation in the pulsed fluidized bed can be simulated by using Eqs. (24), (25) and (32). Fig. 7 is the comparison of the simulated results and the experimental

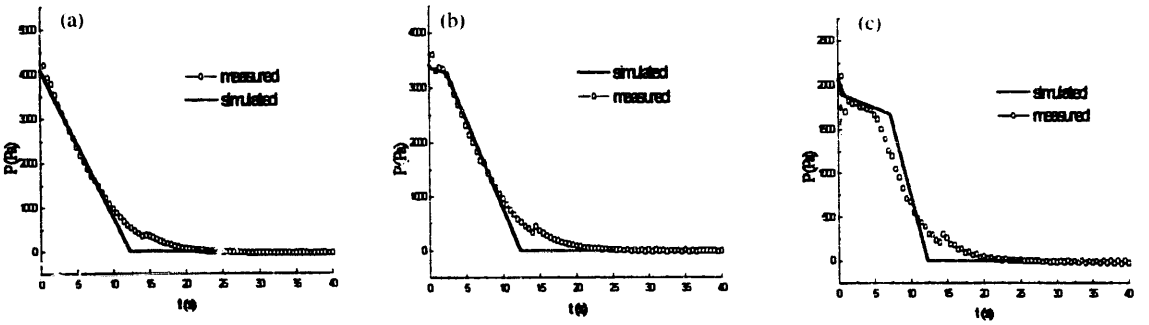

Fig. 6. Comparison between measured and simulated results: (a) near the distributor; (b) 10 cm above the distributor; (c) 30 cm above the distributor.

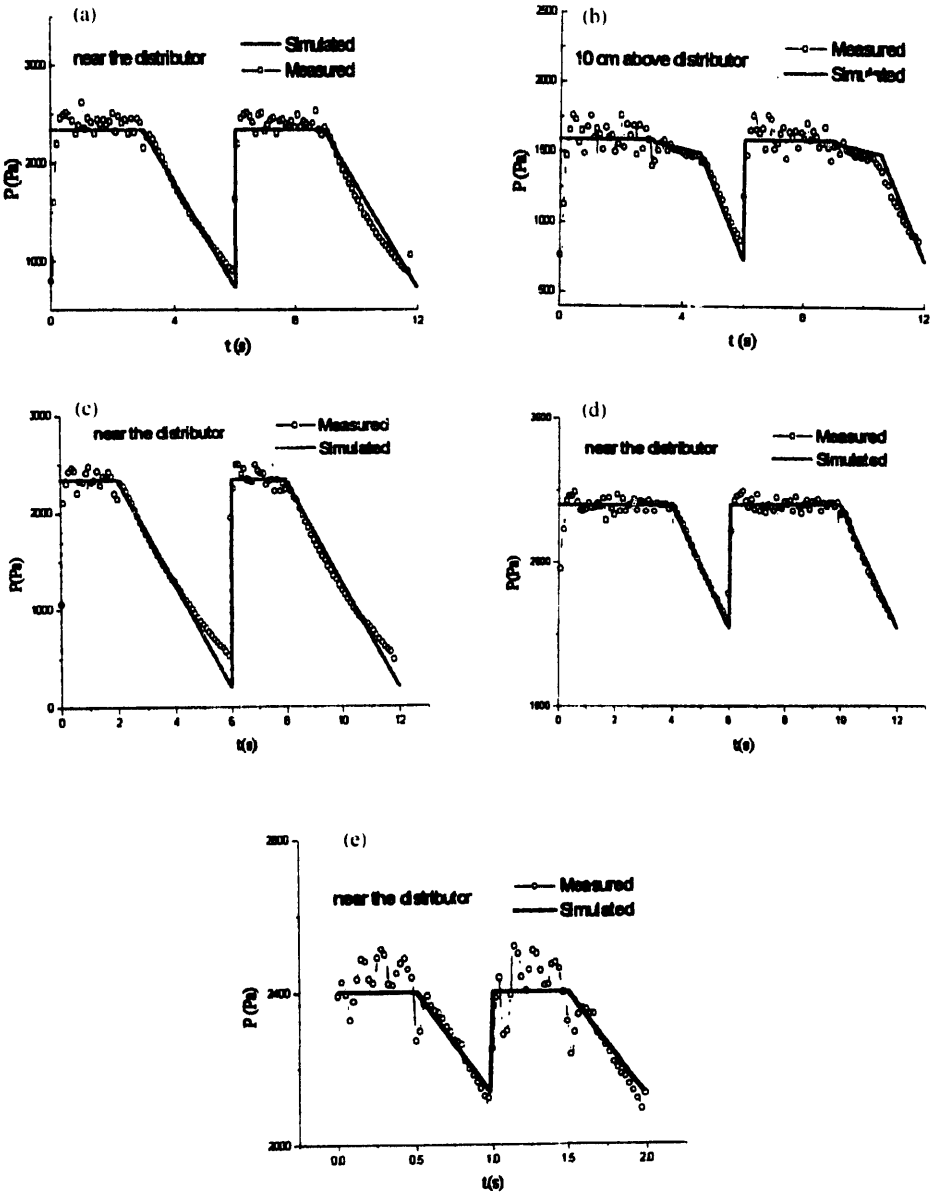

Fig. 7. Comparison between the simulated and measured pressure variation in pulsed bed with different frequency and duration ratio. (a, b) $f = 0.16$ Hz, on-period = 3.0 s, off-period = 3.0 s; (c) $f = 0.16$ Hz, on-period = 2.0 s, off-period = 4.0 s; (d) $f = 0.16$ Hz, on-period = 4.0 s, off-period = 2.0 s; (e) $f = 1.0$ Hz, on-period = 0.5 s, off-period = 0.5 s.

data of pulsed bed with different frequency and duration ratio. We can see that the simulated results are in good agreement with the measured results when the pulse frequency is low.

When the pulse frequency is high, the simplified approach is unsuitable because the effect of the period for establishing steady fluidization can not be neglected.

5. Conclusions

A new method to study the collapsing process of fluidized beds was proposed. The gas-particle flow in fluidized bed was described by a three-phase model (bubble, emulsion and wake), the collapsing process was analyzed and a model was proposed to calculate the pressure variation at different bed location during collapsing. The model was used to simulate the collapsing process and the simulated results are in good agreement with the measured results. The parameters of fluidized beds, such as bubble fraction α_b, particle fraction in dense phase α_p, bubble rising velocity u_b and slip velocity of particle u_t, can be estimated from the experimental data by using the proposed model.

When the pulse frequency is low, the pulsed fluidized bed can be regarded as a combination of a steady fluidization (on-period) and a collapsing process (off-period), the pressure variation can be calculated by Eqs. (24), (25) and (32).

Compared with the conventional method which studies the collapsing process by measuring the bed height variation, recording the pressure variation is a more convenient way to study the collapsing process, furthermore, it can provide more information.

6. Notation

A	sectional area of the bed (m^2)
H_0	initial bed height (m)
H_s	static bed height (Pa)
p	pressure (Pa)
P_a	atmospheric pressure (Pa)
p_{in}	pressure in plenum (Pa)
t_{cr}	critical time (s)
t_{end}	time of the end of the collapsing (s)
u_b	bubble velocity ($m\ s^{-1}$)
u_g	superficial gas velocity ($m\ s^{-1}$)
u_{mf}	initial fluidization velocity ($m\ s^{-1}$)
u_p	particle velocity ($m\ s^{-1}$)
u_t	slip velocity of particles ($m\ s^{-1}$)
V_0	volume of the plenum (m^3)
W	weight of particle in the column (N)
x	coordinate (m)
α_b	bubble fraction
α_p	particle fraction in dense phase
α_w	wake fraction
α_z	particle fraction in settled phase
ρ_p	particle density ($kg\ m^{-3}$)
ΔP_d	pressure drop across distributor (Pa)
μ_g	viscosity coefficient (Pa s)

Acknowledgements

This work is supported by the Multiphase Reaction Laboratory, Institute of Chemical Metallurgy, Chinese Academy

Appendix A

Derivation of Eq. (1)

The continuity equation for particle is:

$$\frac{\partial(\varphi_p\rho_p)}{\partial t}+\frac{\partial(\varphi_p\rho_p U_p)}{\partial x}=0 \tag{a1}$$

Where φ_p is the averaged volume fraction of particle (include the particles in bubble, wake and dense phase), U_p is the averaged velocity of particle.

The continuity equation for gas is:

$$\frac{\partial[(1-\varphi_p)\rho_g]}{\partial t}+\frac{\partial[(1-\varphi_p)\rho_g U_g]}{\partial x}=0 \tag{a2}$$

Where U_g is the averaged velocity of gas.

Because the density of particle and the density of gas are constant, Eqs. (a1) and (a2) can be expressed as:

$$\frac{\partial\varphi_p}{\partial t}+\frac{\partial(\varphi_p U_p)}{\partial x}=0 \tag{a3}$$

$$\frac{\partial(1-\varphi_p)}{\partial t}+\frac{\partial[(1-\varphi_p)U_g]}{\partial x}=0 \tag{a4}$$

Adding Eqs. (a3) and (a4):

$$\frac{\partial[\varphi_p U_p+(1-\varphi_p)U_g]}{\partial x}=0$$

So,

$$\varphi_p U_p+(1-\varphi_p)U_g=\text{constant} \tag{a5}$$

Eq. (a5) can be applied to both steady and unsteady gas–solids flow, including collapse process. For a collapsing fluidized bed,

$$\varphi_p U_p=\alpha_w(1-\varepsilon_w)u_b+(1-\alpha_b-\alpha_w)\alpha_p u_{p,B}(1-\varphi_p)U_g$$

$$=\alpha_b u_b+\alpha_w\varepsilon_w u_b+(1-\alpha_b-\alpha_w)(1-\alpha_p)u_{g,B}$$

Eq. (a5) becomes:

$$\alpha_b u_b+\alpha_w u_b+(1-\alpha_b-\alpha_w)[\alpha_p u_{p,B}+(1-\alpha_p)u_{g,B}] \tag{a6}$$

$$=u_t$$

If the velocity of dense phase is u_e, then

$$\alpha_p u_{p,B}+(1-\alpha_p)u_{g,B}=u_e \tag{a7}$$

Replacing Eq. (a7) into Eq. (a6):

$$\alpha_b u_b+\alpha_w u_b+(1-\alpha_b-\alpha_w)u_e=u_t \tag{a8}$$

Appendix B

Derivation of the pressure distribution during collapsing